

MANUFACTURING AND APPLICATION OF PA11-GLASS FIBER COMPOSITE PARTICLES FOR SELECTIVE LASER SINTERING

Maximilian A. Dechet ^{#*}, Lydia Lanzl ^{†*}, Yannick Werner [#], Dietmar Drummer ^{†*}, Andreas Bück ^{#*}, Wolfgang Peukert ^{#*}, Jochen Schmidt ^{#**}

[#] Institute of Particle Technology (LFG), Friedrich-Alexander-Universität Erlangen-Nürnberg, Cauerstr. 4,
D-91058 Erlangen, Germany

[†] Institute of Polymer Technology, Friedrich-Alexander-Universität Erlangen-Nürnberg, Am Weichselgarten 9,
91058 Erlangen, Germany

[‡] Collaborative Research Center 814 – Additive Manufacturing, Am Weichselgarten 9, D-91058 Erlangen,
Germany

Abstract

Selective laser sintering (SLS), a powder-based additive manufacturing technology, employs micron-sized polymer particles, which are selectively fused by a laser. SLS yields excellent part qualities with good mechanical properties. However, a persistent challenge in this layer-by-layer process is a reduction of mechanical properties in the z-direction. This is often caused by insufficient layer adhesion. One way to strengthen the layer adhesion in z-direction is the incorporation of glass fibers, which exceed from one layer into another. However, most commercially available glass-fiber enhanced materials are dry blends of the polymer powders and the fibers. In order to enhance the isotropic mechanical properties of parts manufactured via selective laser sintering, the manufacturing of glass fiber-filled PA11 particles is shown in this contribution. We present a single-pot approach to produce glass fiber-filled polyamide 11 (PA11) composite particles. The particles are manufactured via liquid-liquid phase separation and precipitation [1] (also known as solution-dissolution process) from ethanol glass fiber dispersions. Bulk polymer material of PA11 is directly converted to composite microparticles in a single process. The produced particles are characterized regarding their size and morphology. The amount of glass fibers in the bulk is assessed via thermogravimetric analysis and the effect of the fibers on the processing window is investigated via differential scanning calorimetry (DSC). As a proof of concept, the powder is employed in the SLS process to produce glass fiber-enhanced test specimens for mechanical testing.

Introduction

Powder-based additive manufacturing technologies, especially laser powder bed fusion (aka. selective laser sintering (SLS)) yields parts of high quality and stability, without the need for support structures. In this process, a homogeneous layer of powder is spread via doctor blade or roller onto a building platform. The particles in the spread powder are selectively fused with a laser, according to the cross section of the part to be built in this layer, before the building platform is lowered by the height one powder layer and the process is repeated. The process is operated at elevated temperatures, namely between the onset of melting and the onset of crystallization, the so called sintering window [1]. The most obvious material requirement is that the feedstock must be a powder. However, the requirements on the material to obtain parts of high quality are much more demanding. Suitable powders must be optimized with regard to their flowability and packing properties, particle size and shape, but also thermal and rheological properties. Therefore, the most widely and most successfully employed material for SLS is polyamide 12 with a market share of around 90%, while the rest is made up of e.g. polyamide 11, polypropylene, PEEK and others [2]. For SLS they show good intrinsic properties (aging behavior, sintering window, crystallization kinetics) rendering them very suitable for SLS [3]. To overcome some of the PA12 or PA11 specific drawbacks, like mediocre mechanical properties, it is possible to add fiber materials to the polymer powder, in order to obtain fiber-reinforced parts with high stiffness for applications like housing in automotive [4]. As fibers might reduce the flowability of a dry blended powder system due to their large diameter-length ratio [5], it is desirable to incorporate the fibers into the polymer particle. By that, process properties, like flowability as well as optical properties of the powder are hardly

influenced by the fillers. A comprehensive overview on advantages and challenges of fiber reinforced additive manufacturing is given in a recent article by Fidan et al. [6].

While the commercially available polyamide 11 is produced via cryogenic grinding, the largest portion of the PA12 powder used in SLS is precipitated using the thermally-induced liquid-liquid phase separation (TIPS), or solution-dissolution, process [3,7]. This process is based in the dissolution of the polymer in a moderate solvent. Such a solvent dissolves the polymer only at elevated temperatures, so that upon cooling the homogenous solution, the solvent cannot dissolve the polymer anymore. Subsequently, during cooling, the system reaches a miscibility gap, where TIPS sets in, dependent on the system composition and process parameters. Droplets of high polymer concentration form in a matrix of high solvent concentration. Consequently, the polymer in the droplets crystallizes or solidifies and polymer microparticles are precipitated. The resulting size distribution and shape are governed, among other parameters, on the polymer-solvent pairing, the polymer concentration, droplet coarsening by coalescence and Ostwald ripening, stirring conditions etc. More information on this process can be found in [8–12].

In a recent publication, we investigated this process for the manufacturing of PA11 particles and performed a thorough particle and material characterization before applying the material in the SLS process, where we could show its processability [13]. The advantage of this process is the possibility to add stabilizers, fillers or other compounds easily during the TIPS process, which get incorporated into the particles. Based on this work, in this study we investigate the manufacturing of glass fiber-filled PA11 particles with a fiber concentration of 25 vol.%. The fiber length distribution of the employed milled glass fiber material is assessed via light microscopy and the particle size distribution (PSD) of the manufactured composite powder is investigated via laser diffraction particle sizing. The incorporation of the glass fibers into the polymer particles, as well as the resulting particle shape, is studied via SEM imaging. The glass content in the manufactured and sieved powder is determined via thermogravimetric analyses. Furthermore, the thermal properties, namely the sintering window, as well as a possible effect of the fiber material on the polymer crystallization, is investigated via DSC. Based on the performed powder characterization, appropriate laser sintering parameters for the manufacturing of test specimens with a desktop laser sintering device could be identified. As a proof of concept, thereby manufactured test specimens made from neat PA11 powder and the glass-filled PA11 composite powder respectively, are mechanically tested to assess the strengthening effect of the glass fibers. The resulting part morphology, especially the fiber distribution in the laser sintered specimens, is investigated via light microscopy on resin embedded cross sections.

Materials

As feed material polyamide 11 granules (Rilsan BMN O natural, Arkema) were used. Ethanol (99.5 %, denatured with 1 % MEK, VWR) was used as a moderate solvent without further purification. The fibers used for filling the PA11 were milled glass fibers of the type OK-7904 FM with a nominal fiber length of 0.2 mm (WELA Handelsgesellschaft mbH).

Methods

Precipitation of glass fiber-filled PA11 particles

DAB-3 (Berghof) steel autoclaves equipped with PTFE liners placed on stirrer hotplates were used as reactors for particle manufacturing. A detailed description of the particle precipitation procedure can be found in [13]. In all reported experiments 18 g PA11 granules and 82 g ethanol were used. Furthermore, in order to obtain a PA11-glass fiber composite material with 25 vol.% of glass fibers, 13.5 g of glass fiber material was added. The autoclaves were then heated to 190 °C, where the system was held for 15 min, to ensure complete dissolution of the PA11, before heating was turned off. The system was then cooled to 130 °C, where an isothermal step was applied for 30 minutes. Stirring inside the autoclaves was realized via magnetic stirring bars (6mm x 25 mm) at 300 rpm. The autoclaves were opened at temperatures below 60°C and the product particles were collected by filtration via a Büchner funnel (Grade 1 filter, Whatman). The recovered wet particles were subsequently dried in an oven and sieved with a 160 µm sieve.

Laser diffraction particle sizing

Particle size distributions (PSDs) of the glass fiber-filled PA11 particles were measured by laser diffraction using a Mastersizer 2000 equipped with a Scirocco 2000 dry dispersion unit (Malvern). The dispersion gas pressure was 2 bar.

Glass fiber size analysis

Since size measurement of fibers is not feasible via laser diffraction, the fiber lengths were measured via light microscopy under 10X magnification with a Morphologi G3 (Malvern). For the measurement, around 60,000 particles are dry-dispersed and then measured optically.

Scanning Electron Microscopy (SEM)

Shape and surface morphology of the PA11 particles were characterized by scanning electron microscopy (SEM) with a GeminiSEM 500 (Carl Zeiss) operated at an acceleration voltage of 1.0 kV. A secondary electron detector was used for imaging.

Differential scanning calorimetry (DSC)

Differential scanning calorimetry (DSC) for the glass fiber-filled PA11 powders was performed using a DSC8000 (PerkinElmer). The samples were placed in standard aluminum pans with covers and measured at a heating rate of 10 K/min from 30°C to 210°C followed by cooling to 30°C at 10 K/min. Measurements were conducted under continuous nitrogen purge gas flow (25 mL/min).

He-pycnometry

Solid density was determined using the helium pycnometer AccuPyc 1330 (Micromeritics) equipped with a 1 cm³ sample cell.

Thermogravimetric analysis (TGA)

Determination of glass fiber content in the filled PA11 powders was realized by measuring the weight of the ash residue via TGA. Experiments were performed in synthetic air using a TGAQ50 (TA Instruments). A ceramic pan with a volume of 250 µl was used and the sample weight was approximately 60 mg. The measurement was conducted in a temperature range of 30–900 °C with a heating rate of 10 K/min. Measurements were conducted once with powder sample mixtures of at least 6 single powder precipitation samples.

Powder bed fusion

To investigate the processability of the manufactured glass-filled PA11 powder in the powder bed fusion process, five test specimens were manufactured on a SnowWhite (Sharebot). The test specimens were tensile specimens according to DIN EN ISO 527-2 type 5A. The device is equipped with a CO₂ laser (wavelength 10.6 µm) with a maximum nominal power of 14 W, the maximum scanning speed is 3500 mm/s and the distance between the laser tip and the powder bed is approx. 20 cm. No information on laser spot size and hatching distance is specified by the device manufacturer. The device is not flushed with nitrogen and operated under air atmosphere. Before and after each experiment, the lens was cleaned with dust-free tissues and absolute ethanol.

Mechanical Testing

All tensile tests were performed on a Z050 (Zwick) tensile testing machine according to DIN EN ISO 527-1. In accordance with the norm, the test speed was 20 mm/min, the clamping length L_0 50 mm and the preload 0.1 N for all samples, to ensure comparability.

Specimen and particle cross section inspection

For analyzing the spatial fiber distribution, cross-sections of the particles and the test specimen are made. The tensile bar and the particles were embedded in epoxy and then grinded and polished. Then, the cross-section of the middle of the tensile bar was analyzed by light microscopy (AxioImagerM2m, Zeiss) under bright field illumination with a magnification of 10x. The prepared particles are analyzed via SEM (Ultra Plus, Zeiss).

Results

To study the manufacturing of glass fiber-filled PA11 particles, it is crucial to obtain information on the fiber length distribution, since the used fiber material is a milled glass fiber powder. While we aim for incorporation of the glass fiber material into the particle matrix, only fibers smaller than the particle can be enclosed fully in the particle matrix. Longer fibers might protrude from the particle and even longer fibers might only be coated by the polymer. In Table 1, the representative number- and volume-weighted fiber length distribution, given as x_{10} , x_{50} , and x_{90} values, as determined via light microscopy are listed.

Table 1: Fiber length distribution

	$x_{10} / \mu\text{m}$	$x_{50} / \mu\text{m}$	$x_{90} / \mu\text{m}$
Number-weighted	1.87	4.45	23.88
Volume-weighted	20.94	66.91	240.3

It is obvious, that the milled fiber material displays a broad length distribution, with a large portion of very small sub $5 \mu\text{m}$ fiber fragments, which are formed during milling. The large number of small fiber fragments is beneficial for filling the particles, as the mean particle size obtained from the precipitation of PA11 from ethanol employing comparable parameters is larger (c.f. $80 \mu\text{m}$ to $130 \mu\text{m}$ [13]). However, the large $x_{90,3}$ length shows, that also very long fibers must be present in the fiber material. The longest observed fiber even measured $571.9 \mu\text{m}$. Such long fibers, while beneficial for macroscopic strengthening, as they extend over several particles or powder layers in the SLS process, can hardly be incorporated into single particles and might negatively influence powder flowability or spreadability and subsequently SLS processability. To assess the incorporation of the glass fiber material and the resulting PA11 composite particle shape and morphology, SEM imaging was conducted. In Figure 1, three representative images are shown.

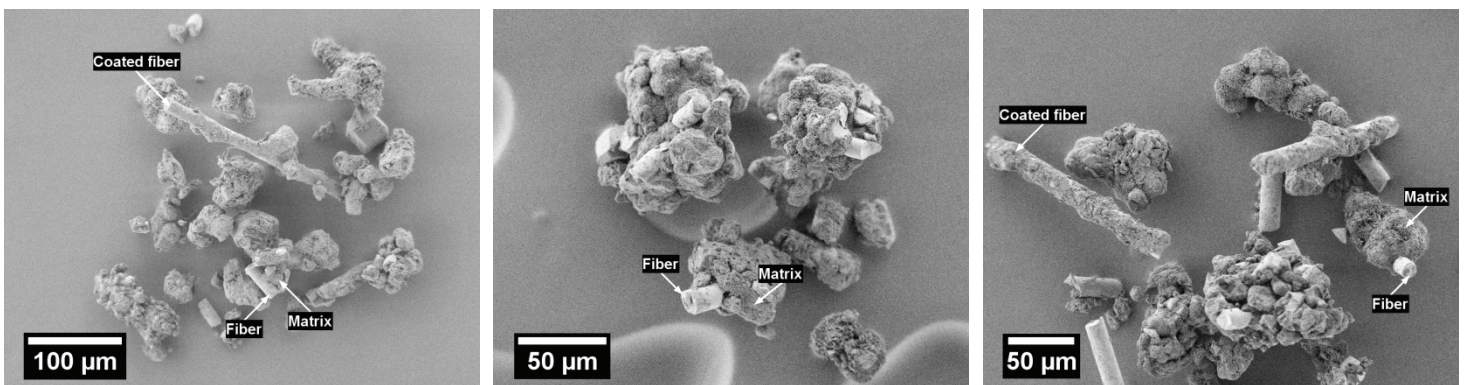


Figure 1: SEM images of the manufactured glass-filled PA11 powder.

The images support the assumptions made based on the fiber lengths distribution. Particles with nearly enclosed or protruding fiber fragments can be identified, as well as larger fibers, which are coated with polymer. Also fibers with particles attached at the end are visible. While these observations prove, that our approach to manufacture PA11-glass fiber composite particles via TIPS is successful, they also show, that employing a

milled glass fiber material leads to a wide variety of particle shapes and sizes, as well as polymer-coated fibers. Coating of fibers with polymer via TIPS for application in SLS has previously been reported by Yang et al. [14], where carbon fibers were coated with PA12. They found enhanced mechanical properties due to the homogeneous distribution of the fibers and the strong interfacial bonding. These effects will be investigated for our PA11 composite powder in the following via mechanical testing and cross-section imaging of parts manufactured via SLS.

However, in order to identify appropriate process parameters for SLS, the particles size distribution of the manufactured particles, which is linked to the applicable layer height in the CAD model and the sintering machine, must be known. In previous studies concerning laser sintering of PA11 particles manufactured via TIPS, we found the removal of a coarse fraction larger than 160 μm to be a viable method to ensure good SLS processability [13]. The volume-weighted particle size distribution of the PA11-glass fiber composite powder is depicted in Figure 2 (left). The powder exposes a mean particle size of 65.4 μm , which is well comparable to commercial SLS powders [3,13,15,16]. With a $x_{10,3}$ of 21.2 μm and a $x_{90,3}$ of 145.7 μm , the fine fraction is smaller and the coarse fraction larger than commercial powders (c.f. non-sieved: $x_{10,3} = 19.8 \mu\text{m}$, $x_{50,3} = 66.0 \mu\text{m}$ and $x_{90,3} = 155.4 \mu\text{m}$). The distribution width, given as span calculated as $(x_{90,3} - x_{10,3})/x_{50,3}$, is 1.9 (c.f. non-sieved: 2.1), indicating a rather broad distribution. However, this could be easily overcome by further removal of fine and coarse fraction via sieving and classification. In this study, we refrain from doing so, as the goal is a proof of principle of the process route to obtain glass fiber-filled PA11 composite particles, which can be employed in SLS, and not optimized material development.

While the SEM images showed, that the incorporation of the glass fibers was successful, no information on the final glass concentration is obtained. To check, if the intended glass fiber concentration of 25 vol.%, added during the initial manufacturing process, is still present in the dried and sieved powder, TGA measurements were performed. The recorded progression of weight loss over temperature is depicted in Figure 2 (right).

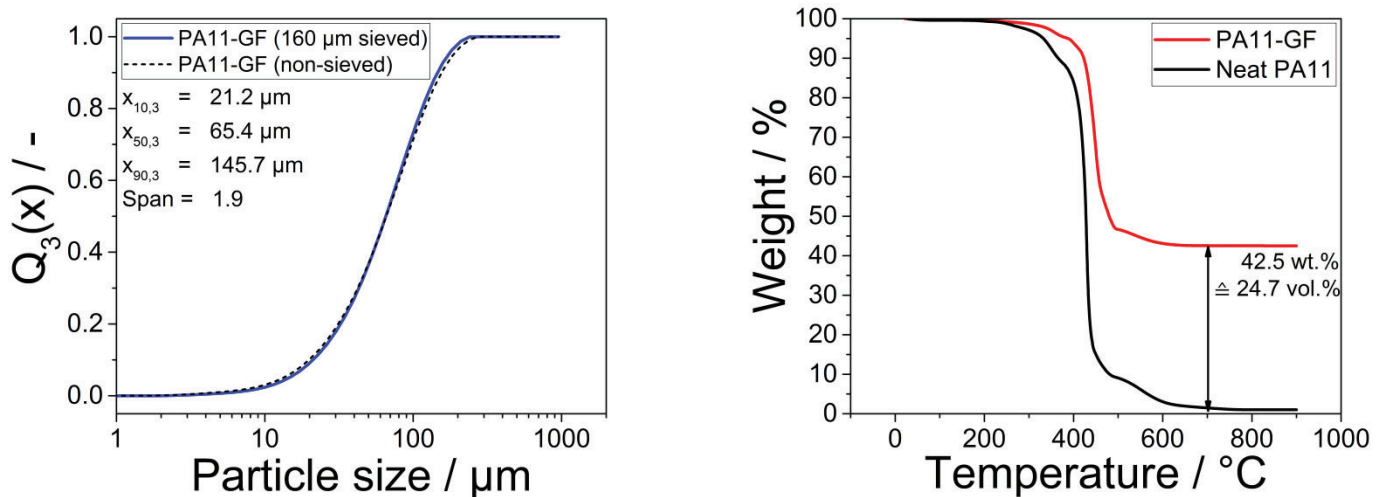


Figure 2: Particle size distributions of the manufactured sieved and non-sieved PA11-glass fiber composite powder (left) and progression of weight loss over temperature as obtained by TGA (right). Onset of degradation is 424 $^{\circ}\text{C}$ for the glass-fiber composite and 415 $^{\circ}\text{C}$ for neat PA11.

The ash residue, which can be correlated to the weight concentration of the glass fibers, was determined to be 42.5 wt.%. With a density, as obtained by He-pycnometry, of 2.598 g/cm^3 and 1.110 g/cm^3 for the glass fiber material and the PA11 particles [13], respectively, the volume concentration of the glass in the powder bulk is 24.7 vol.%. This matches the intended volume concentration of 25 vol.% nearly perfect, even though the bulk powder obtained after the TIPS process was washed, dried and sieved. The powder yield after production and these post processing steps was higher than 90%, rendering the TIPS process and the subsequent post processing quite efficient. The TGA shows, that it is possible to tailor the glass concentration in the PA11-glass fiber composite powder by mere addition of the desired glass content to the initial TIPS process in a one pot approach. Furthermore, the glass reinforced particles exhibit a slightly higher onset of degradation, with 424 $^{\circ}\text{C}$ compared to 415 $^{\circ}\text{C}$ for the neat PA11.

Another important material characteristic, which is crucial for successful SLS processing, is the thermal sintering window, given as the temperature difference between the onset of melting and the onset of crystallization (often determined with heating and cooling rates of 10 K/min). The processing temperature in the building chamber should be in this window, to mitigate premature crystallization of the molten polymer after laser exposure. A thermogram depicting the first heating and cooling of the glass fiber-filled PA11 powder and the appropriate sintering window is displayed in Figure 3.

The displayed thermogram is typical for PA11 particles obtained via TIPS, with the double α -phase melting endotherm and a sintering window in the range of 17 °C to 19 °C [13]. The glass fiber composite material shows an onset of melting at 184.6 °C and an onset of crystallization at 166.3 °C, which corresponds to a sintering window of 18.3 K. The glass fiber material, even though its large number concentration of sub-5 μm fragments, does not act as a nucleating agent causing premature crystallization. Considering the thermal properties of the composite powder, sufficient processability can be expected, as the sintering window is large enough to compensate minor deviations on temperature during processing and the glass fiber material does not affect the crystallization negatively.

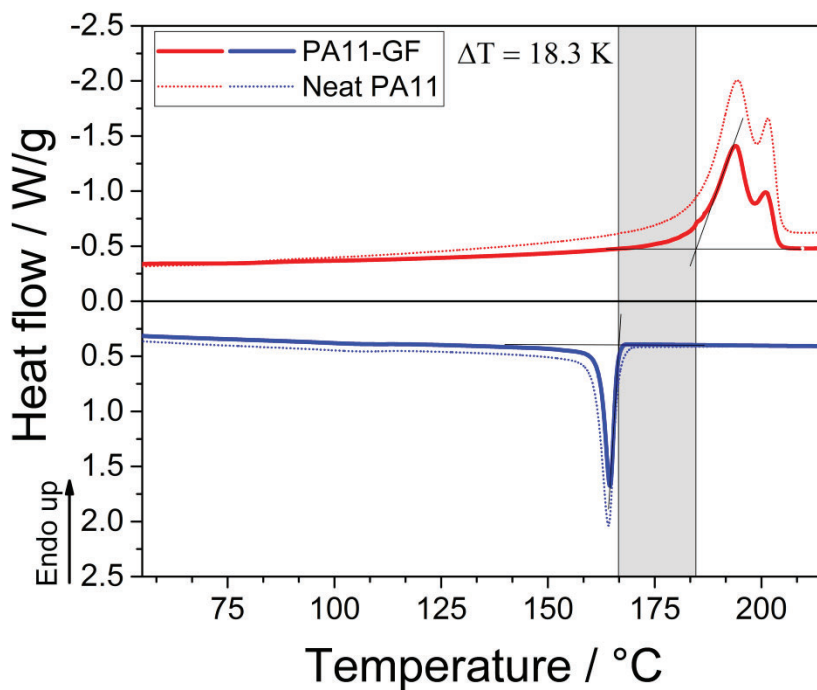


Figure 3: Thermogram of the first heating and cooling cycle of the PA11-glass fiber composite material and neat PA11 material determined with a scanning rate of 10 K/min. The heat flow of the composite material has not been corrected for the mass of glass, thus yielding lower absolute enthalpy as compared to the native PA11 material.

Based on the preceding powder characterization, suitable processing parameters for SLS with the SnowWhite desktop sintering machine can be chosen. In the slicer software, a layer height of 0.3 mm was used, which correlates roughly to twice the $x_{90,3}$, a value often used as rule of thumb. Under consideration of the DSC results, the building chamber temperature, given in the device as environmental temperature, was set to 157 °C, which correlates to a powder bed temperature in the device of approx. 177 °C. Since the glass might absorb some of the laser light and our particles are larger than standard PA12 powder material, we deviate from the processing parameters given by the device manufacturer for sintering of PA12. In Table 2, a comparison between the most important processing parameters given for PA12 and our settings can be found. After a few test runs, sufficient sintering results could be obtained with a laser power of 4.2 W and a scanning rate of 825 mm/s in the bulk and 550 mm/s at the part borders. Furthermore, a waiting time of 20 seconds, after laser illumination and before the next powder layer is deployed, was set.

Table 2: Comparison between the most important processing parameters given for PA12 and the settings employed for sintering of our PA11-glass fiber composite powder.

Material	Standard PA12	PA11-GF composite
Temperature (environmental) / °C	138 - 143	157
Laser power / W	2.8	4.2
Scanning Speed / mm/s	2188	825
Scanning Speed (border) / mm/s	2188	550

These parameters are not optimized and the resulting part qualities are hardly comparable to industrial laser sintering machines. Thorough processing parameter optimization could not be realized, because due to the air atmosphere present in the SnowWhite device and the well-known aging of polyamide powder materials, virgin material was only used once for each experiment. This increased material demand had to be met with the present production rate of 18g polymer material per precipitation experiment. However, we were able to manufacture multi-layered test specimens from our produced PA11-glass fiber composite powder and could show its basic SLS processability.

To assess the effect of the glass fiber material on the part properties, mechanical testing of the manufactured test specimens was conducted. For better comparison, also test specimens manufactured under identical parameters via SLS from neat PA11 powder, produced via TIPS, were investigated. The resulting ultimate tensile strength and elongation at break for the neat PA11 and the PA11-glass fiber composite are listed in Table 3.

Table 3: Mechanical properties of the test specimens manufactured from neat PA11 and PA11-glass fiber composite.

Sample (n = 5)	Ultimate tensile strength / MPa	Elongation at break / %
Neat PA11	7.1 ± 0.5	5.9 ± 0.5
PA11-glass fiber composite	21.4 ± 1.1	6.3 ± 0.2

Even though the mechanical properties, as compared to injection molding or laser sintering with optimized parameters on industrial devices, are rather weak, a strong increase in ultimate tensile strength can be observed for the composite powder. The elongation at break was apparently not affected by the addition of glass fiber material. For the neat PA11 specimens, we observed a fracture behavior governed by delamination, which could explain the weak ultimate tensile strength and the low elongation at break. The employed processing parameters lead to subpar layer adhesion and thus, delamination under tensile stress. This causes the unexpected low elongation at break in the same range as the much more brittle glass fiber composite. For the composite material, the employed manufacturing parameters yield stronger parts without any observed delamination under stress. This could be caused by the longer fibers extending between the layers and thus, linking the layers, which would benefit the layer adhesion. Furthermore, glass absorbs light very well in the CO₂-laser wavelength (10.6 μm) [17]. Since some glass fibers protrude from the polymer particle, they are directly exposed to the laser during illumination, which could increase the effective energy input into the powder bed. This could lead to better sintering and therefore overall increased layer adhesion. Due to the limited amount of material and the temperature-induced ageing of polyamides [18] (especially under air, as it is the case in the desktop sintering device), we refrained from an extended parameter study to identify optimized processing parameters. To study the unaged, pristine powder properties, each powder batch was only used once for laser sintering. Nevertheless, it can be observed, that the fibers strengthen the material, even though they are smaller than typically used fiber material [19,20]. Via mechanical testing, we could show the basic SLS processability of our PA11-glass fiber composite powder and the strengthening effect of the fibers. However, no information on the fiber orientation in the polymer matrix could be gained. Therefore, a small fragment of a previously tested tensile specimen was embedded in epoxy, grinded and polished, until a plane cross section of the laser sintered specimen could be investigated under the light microscope. Images of the analyzed cross sections can be found in Figure 4 (left). Furthermore, a SEM image of the glass-filled particle cross-section is depicted in Figure 4 (right).

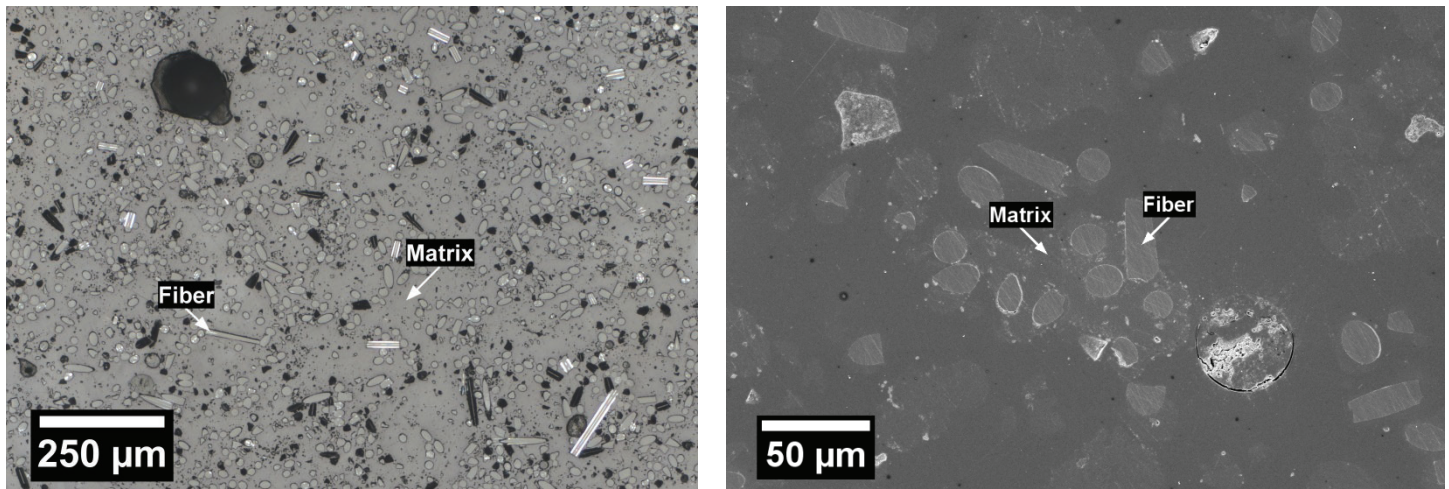


Figure 4: Cross-section of laser sintered specimen made from PA11-glass fiber composite (left). SEM image of PA11-glass fiber composite particle cross sections (right).

The investigated cross sections show, that the glass fibers are distributed homogeneously throughout the part. No segregation effects or one-direction fiber orientation can be detected, which is important for isotropic part properties. In addition, the part exhibits a dense structure, which means that the powder composite offers a high packing density and proper flowability. The black spots in Figure 4 (left) result from sample preparation as some of the fibers fall out during grinding. The inspection of the particle cross sections supports the observation made by SEM imaging of the particles, as glass fiber fragments and glass fibers can be identified in the polymer particle matrix.

Conclusions

In this study, we could show a one-pot approach to manufacture a PA11-glass fiber composite powder based on a TIPS process, where small fiber fragments are incorporated into the polymer particle and larger fibers are coated with the polymer. Furthermore, via TGA we could show, that it is possible to tailor the glass fiber concentration by simply adding the desired amount during the initial TIPS process. Even though the powder was washed and sieved, the measured amount of glass in the composite powder agreed perfectly with the desired amount of 25 vol.%. With a mean particle size 65.4 µm, the manufactured composite powder was in the typical size range for SLS materials, even though the size distribution was not optimized by narrowing via sieving and classification. The DSC analysis showed, that the fiber material does not influence the crystallization and that the composite powder displays a sintering window of 18 °C. Following the powder characterization, processing parameters for laser sintering in the desktop SLS device could be identified, whereby the basic SLS processability of our composite powder could be proven. Though the laser sintering parameters are not optimized yet, a clear strengthening effect of the glass fiber material could be observed for the absolute mechanical properties of the parts. Via light microscopy on cross sections of laser sintered specimens, homogeneous distribution and good adhesion could be shown. For future studies, a thorough comparison between glass-filled PA11 and dry-blended PA11 particle glass fiber mixtures is envisioned, where parts manufactured with optimized sintering parameters in industrial SLS machines are investigated to assess the differences between dry blends and composites.

Acknowledgement

This study has been funded by the Deutsche Forschungsgemeinschaft (DFG, German Research Foundation) – Project-ID 61375930 – SFB 814, Subproject A1, A3 and A6. The financial support is gratefully acknowledged. We thank Franz J. Lanyi and Dirk W. Schubert for performing the mechanical testing.

Literature

- [1] I. Gibson, D. Rosen, B. Stucker, Additive manufacturing technologies, 2. ed., Springer, New York, NY, 2015.
- [2] T.T. Wohlers, Wohlers Report 2016, Wohlers Associates, Fort Collins, Col., 2016.
- [3] M. Schmid, Laser Sintering with Plastics, Carl Hanser Verlag GmbH & Co. KG, München, 2018.
- [4] K. Wudy, L. Lanzl, D. Drummer, Selective laser sintering of filled polymer systems: Bulk properties and laser beam material interaction, *Phys. Procedia*. 83 (2016) 991–1002. doi:10.1016/j.phpro.2016.08.104.
- [5] S. Arai, S. Tsunoda, A. Yamaguchi, T. Ougizawa, Effects of short-glass-fiber content on material and part properties of poly(butylene terephthalate) processed by selective laser sintering, *Addit. Manuf.* 21 (2018). doi:10.1016/j.addma.2018.04.019.
- [6] I. Fidan, A. Imeri, A. Gupta, S. Hasanov, A. Nasirov, A. Elliott, F. Alifui-Segbaya, N. Nanami, The trends and challenges of fiber reinforced additive manufacturing, *Int. J. Adv. Manuf. Technol.* 102 (2019) 1801–1818. doi:10.1007/s00170-018-03269-7.
- [7] S.C. Ligon, R. Liska, J. Stampfl, M. Gurr, R. Mülhaupt, Polymers for 3D Printing and Customized Additive Manufacturing, *Chem. Rev.* 117 (2017) 10212–10290. doi:10.1021/acs.chemrev.7b00074.
- [8] P. van de Witte, P.J. Dijkstra, J.W.A. van den Berg, J. Feijen, Phase separation processes in polymer solutions in relation to membrane formation, *J. Memb. Sci.* 117 (1996) 1–31. doi:10.1016/0376-7388(96)00088-9.
- [9] K.S. McGuire, A. Laxminarayan, D.R. Lloyd, Kinetics of droplet growth in liquid-liquid phase separation of polymer-diluent systems: experimental results, *Polymer*. 36 (1995) 4951–4960. doi:10.1016/0032-3861(96)81620-X.
- [10] S. Kloos, M.A. Dechet, W. Peukert, J. Schmidt, Production of spherical semi-crystalline polycarbonate microparticles for Additive Manufacturing by liquid-liquid phase separation, *Powder Technol.* 335 (2018). doi:10.1016/j.powtec.2018.05.005.
- [11] H. Matsuyama, M. Teramoto, M. Kuwana, Y. Kitamura, Formation of polypropylene particles via thermally induced phase separation, *Polymer*. 41 (2000) 8673–8679. doi:10.1016/S0032-3861(00)00268-8.
- [12] S.-J. Wang, J.-Y. Liu, L.-Q. Chu, H. Zou, S.-J. Zhang, C.-J. Wu, Preparation of polypropylene microspheres for selective laser sintering via thermal-induced phase separation: Roles of liquid-liquid phase separation and crystallization, *J. Polym. Sci. Part B Polym. Phys.* 55 (2017) 320–329. doi:10.1002/polb.24275.
- [13] M.A. Dechet, A. Goblirsch, S. Romeis, M. Zhao, F.J. Lanyi, J. Kaschta, D.W. Schubert, D. Drummer, W. Peukert, J. Schmidt, Production of polyamide 11 microparticles for Additive Manufacturing by liquid-liquid phase separation and precipitation, *Chem. Eng. Sci.* 197 (2019) 11–25. doi:10.1016/j.ces.2018.11.051.
- [14] C. Yan, L. Hao, L. Xu, Y. Shi, Preparation, characterisation and processing of carbon fibre/polyamide-12 composites for selective laser sintering, *Compos. Sci. Technol.* 71 (2011) 1834–1841. doi:10.1016/j.compscitech.2011.08.013.
- [15] J. Schmidt, M. Sachs, S. Faselow, M. Zhao, S. Romeis, D. Drummer, K.E. Wirth, W. Peukert, Optimized polybutylene terephthalate powders for selective laser beam melting, *Chem. Eng. Sci.* 156 (2016) 1–10. doi:10.1016/j.ces.2016.09.009.
- [16] M. Schmid, A. Amado, K. Wegener, Polymer powders for selective laser sintering (SLS), *Proc. PPS-30 30th Int. Conf. Polym. Process. Soc. – Conf. Pap.* (2015) 160009. doi:10.1063/1.4918516.
- [17] C. Brecher, M. Emonts, R.L. Schares, J. Stimpfl, CO₂-laser-assisted processing of glass fiber-reinforced thermoplastic composites, *High-Power Laser Mater. Process. Lasers, Beam Deliv. Diagnostics, Appl. II*. 8603 (2013) 86030H. doi:10.1117/12.1000243.
- [18] K. Wudy, D. Drummer, Aging Behavior of Polyamide 12: Interrelation between Bulk Characteristics and Part Properties, in: 2016 Proc. 26th Annu. Int. Solid Free. Fabr. Symp., 2016: pp. 770–781.
- [19] S.-Y. Fu, B. Lauke, E. Mäder, C.-Y. Yue, X. Hu, Tensile properties of short-glass-fiber- and short-carbon-fiber-reinforced polypropylene composites, *Compos. Part A Appl. Sci. Manuf.* 31 (2000) 1117–1125. doi:10.1016/S1359-835X(00)00068-3.
- [20] S. Fu, Effects of fiber length and fiber orientation distributions on the tensile strength of short-fiber-reinforced polymers, *Compos. Sci. Technol.* 56 (1996) 1179–1190. doi:10.1016/S0266-3538(96)00072-3.